PHYSICAL REVIEW B **83**, 035117 (2011)

Electron correlation decides the stability of cubic versus hexagonal boron nitride

Migen Halo,[1] Cesare Pisani,[1] Lorenzo Maschio,[1] Silvia Casassa,[1] Martin Schütz,[2] and Denis Usvyat[2]
[1]*Dipartimento di Chimica IFM, and Centre of Excellence NIS (Nanostructured Interfaces and Surfaces), Università di Torino, via Giuria 5, I-10125 Torino, Italy*
[2]*Institute for Physical and Theoretical Chemistry, Universität Regensburg, Universitätsstrasse 31, D-93040 Regensburg, Germany*
(Received 9 December 2010; published 19 January 2011)

Periodic local Møller-Plesset second-order perturbation theory (MP2) is applied to investigate the structural and energetic properties of the cubic and hexagonal polymorphs of boron nitride. While the Hartree-Fock (HF) solution significantly underbinds both systems and energetically favors *h*-BN, the post-HF correlation treatment recovers the lacking amount of the interaction energy and reverts the sign of the relative stability between the two compounds. It provides the physically correct picture and predicts cohesive energies, lattice constants, bulk moduli, and the relative stability in good agreement with experiment. Density-functional theory (DFT) results, on the other hand, are inconclusive and exhibit a strong dependence on the chosen functional. The results of MP2 as well as DFT with an empirical dispersion correction indicate that the dispersion contribution to binding is essential not only for the layered polymorph, but also (and even more so) for the cubic one.

DOI: 10.1103/PhysRevB.83.035117 PACS number(s): 71.15.Nc

I. INTRODUCTION

The zinc-blende-like cubic phase of boron nitride (*c*-BN) has attracted wide attention since its synthesis by Wentorf in 1957[1] due to its outstanding physical and chemical properties, such as extreme hardness, high melting temperature and thermal conductivity, wide band gap, low dielectric constant,[2] chemical inertness[3] (in contrast to diamond, it is stable against oxidation and acid resistant), which make it very attractive for applications in microelectronics, optoelectronics, as a protective-coating material, etc.[1,4] Another polymorph of boron nitride, the graphite-like hexagonal phase (*h*-BN), has recently gained new importance since it represents the fundamental structure of BN nanotubes, the structural analog of carbon nanotubes.[5–7]

These interesting properties have motivated a lot of theoretical and experimental activity. One of the debated issues is the relative stability of the two polymorphs. Until the late 1980s *h*-BN was believed to be the thermodynamically stable phase in standard conditions, the situation being reversed at high pressure, in analogy with the graphite and diamond phases of carbon[8]; this premise was supported by the fact that BN synthesis usually results in the formation of *h*-BN. However, recent updates and refinements of previous measurements by Solozhenko[9,10] have resulted in the opposite conclusion which is now generally accepted, namely, that at zero pressure *c*-BN is the thermodynamically stable phase up to relatively high temperatures, even though the difference in stability has not been reported.

This result is supported by most density-functional theory (DFT) studies,[11–16] which found differences of 3.6 to 6.6 mHa per formula unit in favor of *c*-BN. There are, however, exceptions: Ahmed *et al.*[17] recently estimated *h*-BN to be more stable than *c*-BN by about 6 and 25 mHa according to generalized gradient approximation (GGA) or local-density approximation (LDA) calculations, respectively, the same indication coming from a recent GGA study;[18] according to Janotti,[19] the relative stability depends on the exchange-correlation functional employed, with LDA favoring *c*-BN and GGA favoring *h*-BN, by 5.5 mHa; finally, according to Xu's orthogonal linear combination of atomic orbitals LDA calculations, *h*-BN is favored by 26 mHa.[20] Two nonstandard DFT approaches have been applied recently to several layered compounds, including *h*-BN. Rydberg *et al.*[21] have added to a standard LDA exchange-correlation functional a nonlocal one based on first principles. Madsen *et al.*[22] have used instead a meta-GGA density functional which includes the kinetic-energy density in its expression.[23] The experimental geometry of *h*-BN is well reproduced in both studies, but the case of *c*-BN has not been considered.

The variety of these outcomes is not surprising if one considers the profoundly different structure of the two phases and the intrinsic limitations of DFT schemes. *c*-BN is a dense phase with sp^3 hybridized B-N bonds. On the other hand, *h*-BN is a low-density phase which resembles graphite in that it has a layered structure with strong sp^2 hybridized bonds within the sheets and weak van der Waals–like interactions between them (unlike graphite, however, the layers are arranged in such a way that N and B positions match each other in neighboring sheets). The notorious inability of standard DFT to describe the long-range correlation effects in fact hinders the possibility to capture the correct physics in extended systems, especially so when weak binding is involved. A serious warning about the reliability of DFT techniques in predicting the relative stability of crystalline allotropes comes from a recent study by Demichelis *et al.*[24] Within the same computational scheme, the performance of 12 DFT functionals was there assessed as concerns the equilibrium structure and the relative stability of three aluminosilicates and four aluminum hydroxides. Without entering into details, the results were shown to depend strongly on the exchange-correlation functional used. Standard LDA, GGA, and hybrid schemes were unable to reproduce the correct order of stabilities, which was instead obtained with new functionals like PBEsol,[25] SOGGA,[26] and WC,[27] specially devised for solids which, however, overstabilize the denser phases. As concerns equilibrium geometries, both the standard and the new potentials perform unsatisfactorily for the hydroxides, mainly due to the poor description of H bonds, while hybrid functionals give the best results in this respect. The present case seems even more critical, since van der

Waals interactions play a very important role in *h*-BN; in this respect, hybrid-exchange schemes cannot be of much help, since the Hartree-Fock (HF) approximation suffers from the same inadequacy.

A more general approach is needed treating short- and long-range correlation among electrons in crystals on the same footing. This is precisely the case with the technique here adopted, namely Møller-Plesset theory at second order (MP2), which represents the lowest level of Rayleigh-Schrödinger many-body perturbation theory. The zeroth-order reference within the Møller-Plesset partitioning is the Hartree-Fock solution, and the arbitrariness of the choice of the effective Hamiltonian, inherent in DFT, is therefore avoided. The MP2 correlation correction per unit cell is evaluated by means of the CRYSCOR code[28,29] which adopts the periodic local-correlation technique.[30,31] The fully periodic treatment circumvents the difficult and nonunique modeling of finite clusters and embedding, necessary, e.g., in the context of the incremental scheme.[32–35] MP2 is considered to be an accurate method for nonconducting systems, as has been recently demonstrated[36,37] on a wide variety of crystals. The random-phase approximation based on the DFT reference[38] has been reported to provide similar accuracy. However, its sensitivity to the underlying functional and the neglect of exchange-like[39] terms still remain a matter of debate.

For comparison, the standard DFT approach with three functionals is considered here: two GGAs, i.e., PBE[40] and PBEsol[25] (the latter specially designed for solid-state applications), and a hybrid-exchange PBE0[42] functional. In addition, the dispersion-corrected version of PBE, employing the empirical Grimme correction *D*,[41] has been included in this study.

The outline of this paper is as follows. In Sec. II the computational techniques are described, with special attention given to the choice of the basis sets (BSs) and to the evaluation of the basis set superposition error (BSSE). In Sec. III A the calculated structural and cohesive properties are summarized and discussed. In Sec. III B the importance of the different types of bi-excitations which contribute to the correlation energy is analyzed. The main conclusions are finally drawn in Sec. IV.

II. COMPUTATIONAL TECHNIQUES

A. One-electron calculations

As was mentioned in the Introduction, four variants of PBE-based functionals are considered: PBE,[40] PBEsol,[25] PBE-*D*,[41] which contains an empirical long-range dispersion correction proposed by Grimme, and a hybrid-exchange PBE0.[42] For these DFT calculations, as well as for the computation of the HF reference wave function, the CRYSTAL program was employed. All the calculations use BSs of localized Gaussian-type orbitals (GTOs) centered in the nuclei, to be referred to below also as atomic orbitals (AOs). The delicate issue of the calibration of the BSs is discussed in detail below (Sec. II C). All other computational parameters in CRYSTAL, which control the truncation of the infinite lattice sums, the numerical integration required in DFT calculations for the reconstruction of the exchange-correlation potential, and the sampling in reciprocal space, have been set to very tight values. As concerns the last point, shrinking factors of 12,12,12 for *c*-BN and 12,12,4 for *h*-BN were used, corresponding to 72 and 133 **k** points in the irreducible part of the Brillouin zone, respectively. The TOLINTEG parameters which control the truncation of the Coulomb and exchange lattice series in CRYSTAL[43] have been set to the tight 7,7,7,15,50 values.

From the HF solution expressed in terms of crystalline orbitals, CRYSTAL constructs an equivalent representation of the occupied manifold in terms of Wannier functions (WFs). WFs form a set of orthonormal, translationally equivalent, very localized, and site-symmetry adapted functions,[44,45] which are an essential ingredient for the local correlation scheme (see Sec. II B). The shape and characteristics of the WFs in the present application will be analyzed in Sec. III B 1 it is shown there that for both phases they are centered on an N atom or close to an N atom slightly shifted along the N-B bond.

B. Local periodic MP2 calculations

As just stated, CRYSCOR receives from CRYSTAL all information about the WFs (to be labeled as $i, j, \ldots$). Since the correlation treatment is limited to valence electrons, there are here only four WFs per cell, which span on the whole the same manifold as the four HF valence bands. Following Pulay and Saebø,[30] another set of local functions is used in CRYSCOR to describe the virtual HF space, obtained by projecting each GTO of the BS onto the virtual manifold. The projected AOs (PAOs) (labeled as $a, b, \ldots$) constitute a translationally invariant nonorthogonal (and even redundant) set. The MP2 energy $E^{(2)}$ can be written as a sum of all contributions E_{ij}^{ab}, each corresponding to a two-electron excitation from a pair of WFs to a pair of PAOs, $[(ij) \uparrow\uparrow (ab)]$. The excitation amplitudes are calculated by solving the LMP2 equations.[28] We will refer to "pair energy" as the quantity $E_{ij}^{(2)} = \sum_{ab} E_{ij}^{ab}$, that is, the sum of all the contributions to the correlation energy due to excitations from a given pair (i, j) of WFs. Exploitation of translational symmetry allows us to impose the first WF (i) to belong to the reference zero cell. The local-correlation Ansatz restricts the virtual space for a given (i, j) pair to the PAOs centered in the vicinity of either of the WFs. More precisely, to any given WF (i) a *domain* $\mathcal{D}_i$ is associated consisting of a certain number of atoms close to it. In *c*-BN, eight-atom domains are adopted: $N_3B^*N^*B_3$, the two starred atoms identifying the bond along which the WF is located. In *h*-BN, ten-atom domains are used: $N^*(N_2B)_3$, all atoms lying in the same layer and the starred nitrogen being the one closest to the WF center. Two WFs then define a *pair-domain* $\mathcal{D}_{(ij)}$ which is simply the union of the corresponding domains. Only those $[(ij) \uparrow\uparrow (ab)]$ excitations are retained for which, first, both PAOs a and b belong to atoms in $\mathcal{D}_{(ij)}$, and second, the distance d_{ij} between the centers of the two WFs is within a certain value D. In the present application, D is set to 10 Å for both phases.

Once the relevant WF-PAO pairs are selected, the two-electron repulsion integrals (ERIs), $(ia|jb)$, between the respective product distributions are evaluated. Analytical calculation of ERIs is expensive, therefore approximate techniques are used: local-density fitting,[46,47] for the integrals with

inter-WF distance smaller than 8 Å, and multipole expansions for the rest.

C. Basis set choice and BSSE estimate

In the present study we employ two GTO BSs, namely a triple-ζ polarized set as proposed by Grüneich and Hess,[48] and a modification thereof with the addition of high angular momentum functions, to be referred to in the following as BSA and BSB, respectively. The authors claim that the BSA, which was specially designed for hexagonal BN, is close to the HF limit, since it is able to describe the repulsive behavior of the intersheet interaction energy versus distance without any BSSE correction (poorer BSs provide instead a spurious minimum). This basis contains only one d function per atom. This is generally not sufficient for post-HF calculations, where a number of diffuse high angular momentum functions are required in order to describe accurately the Coulomb hole. Therefore the BSB set contains two d and one f shell per atom; the exponents are taken from the standard cc-pVTZ set of Dunning,[49] without alteration for nitrogen, while for boron the exponents have been roughly optimized to achieve convergence at the HF level (the values of 1.2, 0.6, and 1.0 a.u. for the two d and the f polarization function exponents have been so obtained).

Further improvement of the basis set is possible (using, e.g., the dual basis set scheme[50]), but difficult, because of intrinsic limitations (no AOs with $\ell \geqslant 4$ are possible with CRYSTAL calculations presently), substantial increase of the computational cost, and due to an onset of uncontrollable linear dependencies among diffuse functions, which cause numerical instabilities without actual improvement of the correlation description.[50,51] Nevertheless, as demonstrated below, the BSB set allows for a sufficiently accurate description of the systems studied here.

Even if the basis set superposition error is expected to be small for the sets employed in this work (note that local correlation approaches to a large extent avoid such contamination[52]), all results provided below are corrected for this error according to the standard counterpoise method.[53] That is, cohesive energies are calculated by taking in each case the energies of the individual atoms (B or N) surrounded by ghosts up to second neighbors as the reference. The corresponding restricted open-shell MP2 calculations have been performed with the MOLPRO program package.[54]

III. RESULTS AND DISCUSSION

A. Structural and cohesive properties

Table I provides a summary of all calculated data vs the available experimental ones, while Fig. 1 displays the dependence of the cohesive energy E_0 on geometry for the two phases as resulting from the HF + MP2 (left panel) and DFT calculations (right panel). Here and in the following, E_0 is defined as the difference between the total energy of the crystal *per formula unit* and that of the two isolated atoms with their surrounding ghosts.

From the results reported in Table I it appears that at the HF level of approximation the hexagonal phase turns out to be more stable than the cubic one, at variance with the experiment; the cohesive energy is underestimated by more than 0.1 Ha. It is also clear that basis set effects are here almost negligible, both as concerns the absolute cohesive energy and the relative stability of the two phases. While the HF approximation accurately reproduces the geometry of c-BN and of the individual layers of the hexagonal phase, it cannot account for the interlayer binding in the latter system; in fact, it predicts that h-BN would exfoliate, and correspondingly the bulk modulus cannot be estimated. Adding the MP2 correction has dramatic effects, as shown also in the left panel of Fig. 1.

TABLE I. Structural, cohesive, and elastic properties of c-BN and h-BN. Energy data are per formula unit; data in parentheses give the calculated stability of c-BN with respect to h-BN. Except when indicated, the calculated data were obtained with BSB. Experimental values are taken from Ref. 14, except for the very recent experimental estimate of the bulk modulus of h-BN ($B = 20 \pm 2$ GPa, Ref. 55). For the experimental cohesive energy of c-BN, the zero-point-corrected value is also given (after the slash).

Phase	Technique	V (Å^3)	a (Å)	c (Å)	E_0 (ΔE_0) (mHa)	B (GPa)
c-BN	PBE0	46.43	3.594		−503.7(1.9)	408
	PBE	47.53	3.622		−511.6(4.5)	374
	PBEsol	46.79	3.603		−545.5(−3.1)	389
	PBE-D	47.04	3.610		−534.2(−9.6)	385
	HF	46.53	3.597		−353.4(16.7)	434
	MP2 + HF (BSA)	47.22	3.614		−473.8(−2.6)	392
	MP2 + HF (BSB)	46.46	3.595		−499.6(−6.6)	411
	Expt.	47.43	3.620		−485.0/−492.2 (<0)	369–400
h-BN	PBE0	77.76	2.494	7.218	−505.5	8
	PBE	80.24	2.511	7.347	−516.0	9
	PBEsol	74.03	2.503	6.822	−542.4	10
	PBE-D	66.28	2.497	6.137	−524.6	34
	HF		2.490	> 8.	−370.2	
	MP2 + HF (BSA)	74.15	2.505	6.822	−471.3	12
	MP2 + HF (BSB)	70.12	2.497	6.493	−493.1	24
	Expt.	72.15	2.501	6.66		20–37

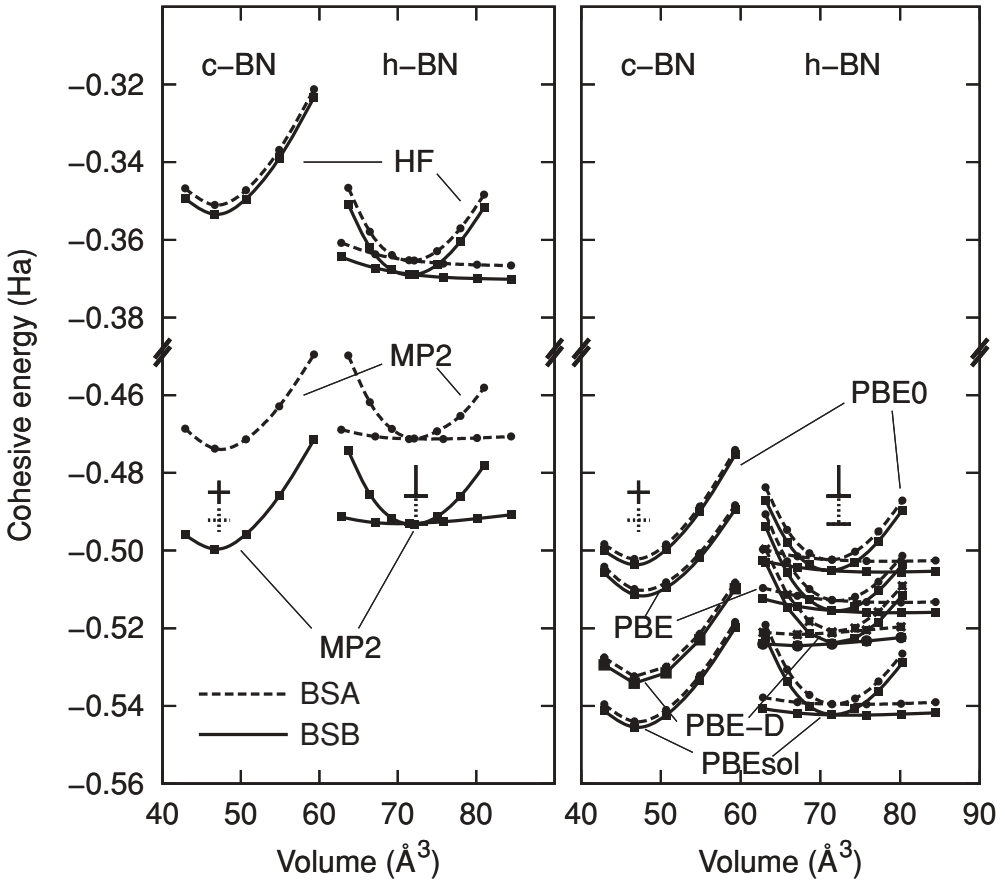

FIG. 1. Calculated energy vs volume data for *c*-BN (on the left of each plot) and *h*-BN (on the right of each plot). The left panel refers to HF + MP2 calculations performed with BSA (dashed line) or BSB (continuous line), the right panel refers to DFT calculations with four functionals as indicated. For *h*-BN two curves are drawn in each case: the shallower one corresponds to changing *c* with *a* fixed at its experimental minimum (which in any case appears to be the minimum for all the methods applied, within ± 0.01 Å), the other one vice versa. The cross marks the best experimental estimate available for *c*-BN. For *h*-BN, the vertical segment marks the position of the experimental volume and a rough estimate of the cohesive energy. The dotted symbols indicate the zero-point energy (ZPE)-corrected values. For other explanations see text.

The basis set effect is seen to be much more important here than in the HF case: the additional *d* and *f* polarization functions in BSB clearly improve the quality of the correlation treatment. Nevertheless, for both sets the correct order of stabilities is restored, which is surprising, in a sense, since it could have been expected that electron correlation primarily would further stabilize *h*-BN due to the inclusion of van der Waals interlayer interactions, which are missing in the HF description. Yet the opposite happens: The energy gain due to the strengthening of the binding in *c*-BN by electron correlation is even larger. The cohesive energy is reproduced almost correctly at the MP2 level in the bigger basis, provided that also zero-point energy corrections are included (*vide infra*). Even more importantly, the MP2 correction provides a satisfactory description of the interlayer binding in *h*-BN. The equilibrium *c* parameter is accurately evaluated, and the interlayer interaction energy, calculated as the difference per formula unit between *h*-BN at equilibrium and the isolated layer, turns out to be 2.4 mHa with both sets, in reasonable agreement with the estimate of 2 mHa obtained by Rydberg *et al.*[21] using the nonlocal DFT approach, specially devised for layered systems.

The data just presented can be compared to the corresponding DFT results collected in Table I and on the right panel of Fig. 1. In some respects the latter are similar to the HF ones: The basis set effects are almost negligible, and the interlayer interaction in *h*-BN is incorrectly reproduced, resulting in too large *c* values. Two of them also wrongly predict *h*-BN to be slightly more stable than *c*-BN, while PBEsol favors as usual the denser phase, so providing the right indication. The calculated cohesive energy itself depends severely on the chosen DFT functional, such that the PBE result is not very far from experiment, while the PBEsol overestimation is substantial.

An important piece of information is delivered by the empirically corrected PBE-*D* method, especially when compared to the underlying PBE. Although the evaluated cohesive energy is not as close to the experiment, PBE-*D* reverts the order of the stability of the phases, predicted by PBE. This is quite a surprising outcome, since the dispersion contribution is anticipated to be crucial for the layered hexagonal structure, and not so much for the three-dimensional-covalent cubic phase. In fact, this is not true, and taking into account the MP2 results, one can conclude that dispersion is essential not only

in the weakly bound systems, but also in the dense covalent (or ionic) solids. Moreover, it can become decisive for the relative stability of the competing phases.

Yet, the general predictive power of the empirical DFT-*D* method remains questionable. For example, in our calculations it severely underestimates the *c*-lattice parameter of the hexagonal polymorph, altering considerably the bare PBE treatment. We believe that this originates from the empirical nature of the added *D* potential, more precisely from the ambiguity of the damping function, which switches off the *D*-correction at close interatomic distances. The damping function is assumed to be spherical depending on the van der Waals radii of the atoms, which might be quite a crude approximation for the system it is applied to and can thus cause unphysical contamination of the potential surface at short range.

The following further comments can be put forward. The relative stability and, to a lesser extent, the cohesive energy are critically dependent on the adopted theoretical scheme. In this respect also the value of −471.2 mHa for the cohesive energy of *c*-BN as obtained from the Monte Carlo study by Malatesta *et al.*[56] should be mentioned. The bulk modulus of *c*-BN, on the one hand, is rather well described by all calculations (but note a certain overestimation by HF, which is known to exaggerate the rigidity of chemical bonds). On the other hand, for *h*-BN this quantity is much more difficult to calculate, since it is essentially determined by interlayer interactions. Hence only the MP2 method in the bigger basis and to a certain extent PBE-*D* can provide a reasonably accurate value.

All the discussion and the results provided so far have not taken into account the zero-point energy correction, the treatment of which becomes mandatory when looking for relative stabilities. We have estimated this quantity in the harmonic approximation by calculating the Γ-point phonons with the CRYSTAL code and using the PBEsol DFT functional. Values of 7.223 and 8.182 mHa per formula unit are so obtained for the ZPE of *c*-BN and *h*-BN, respectively. The difference is less than 1 mHa, and practically coincides with that obtained in previous theoretical studies.[14,15] Inclusion of the zero-point correction virtually does not affect the relative stability. However, the ZPE corrected experimental energies are now quite close to the MP2 BSB cohesive energies.

1. Basis set incompleteness

The MP2 correlation treatment with the bigger basis set BSB provides a reliable description of the electronic structure. The excellent agreement with the experimental cohesive energy in this case is to be taken cautiously, since at the basis set limit the discrepancy may be larger. However, since BSB is already a rather extended set, the basis set limit results should not substantially differ from the BSB ones, which very well fit into the general picture of the MP2 performance. Indeed, for a low-order perturbative correlation method a slight overestimation of the interaction energy at the basis set limit is common. Besides, despite the noticeable improvement of the cohesive energies achieved by using the BSB, the form of the potential surface and the relative stability are substantially less affected by the choice of the basis.

As mentioned in Sec. II C, a further expansion of the basis set in order to approach that limit or to make an extrapolation to it is presently unfeasible. The main difficulties come from the relatively diffuse functions present in the balanced high quality molecular basis sets, which cause numerical problems in the periodic case.

Another problem one has to deal with when the basis set is not close to completeness is the BSSE. With our basis sets, the BSSE at the HF level and for all DFT calculations is totally negligible (less than 0.5% of the cohesive energy value), while at the MP2 level it becomes relatively important. It amounts to 8% (11%) and 10% (13%) of the cohesive energy for *c*-BN and *h*-BN, respectively, with BSB (BSA). This error is basically due to the bad description of the B atom, which indeed improves significantly when enriching the basis set, while the N atom seems insensitive to it; the BS dependence of the BSSE is similar for the two phases.

B. Analysis of the MP2 energy

1. Characteristics of Wannier functions

Figure 2 shows the shape of the WFs for the two phases, while Table II reports some of their characteristic parameters; the nomenclature adopted for identifying them is evident from there. These data were obtained with BSB, but they are practically coinciding with the BSA ones. It can be observed that all WFs are rather well localized, their spread R_i being comparable to the B-N bond length (1.472 and 1.443 Å for *c*-BN and *h*-BN, respectively). Also note that, due to their symmetry characteristics, none of *c*-BN WFs are localized on the N atom, in contrast to the other phase.

For each WF, the value $\overline{f}_i$ is also indicated, which measures the minimum energy required, in the Koopmans theorem sense, to remove an electron from this orbital (for the sake of reference, we report the values of the HF band gaps, which are almost the same with the two BSs: 0.506 Ha for *c*-BN, 0.502 Ha for *h*-BN). The different WFs lend themselves to a rather simple chemical interpretation, which will simplify the analysis of the different contributions to the correlation energy to be performed in Sec. III B 2. The symmetry unique WF of the cubic phase, w^c, is essentially an sp^3 hybrid of

TABLE II. Characteristic parameters of the symmetry-independent WFs for the two phases. $R_i = [\int d\mathbf{r} w_i(\mathbf{r})^2(\mathbf{r}-\mathbf{C}_i)^2]^{1/2}$ is a measure of the spread of the ith WF about its centroid $\mathbf{C}_i$; δ_i is the distance of $\mathbf{C}_i$ from the nearest N atom; $\overline{f}_i = \langle w_i|\hat{f}|w_i\rangle$ is the expectation value of the Fock Hamiltonian with reference to the bottom of the conduction bands. The symmetry subgroup and the irrep are indicated, while n_{eq} gives the number of rotationally equivalent functions in the reference cell.

Phase	WF	R_i (Å)	δ_i (Å)	$\overline{f}_i$ (mHa)	Symmetry	(n_{eq})
c-BN	w^c	1.50	0.526	−897	C_{3v}/A_1	(4)
	w_1^h	1.38	0.	−1289	D_{3h}/A_1'	(1)
h-BN	w_2^h	1.71	0.126	−781	D_{3h}/E'	(2)
	w_3^h	1.43	0.	−609	D_{3h}/A_1''	(1)

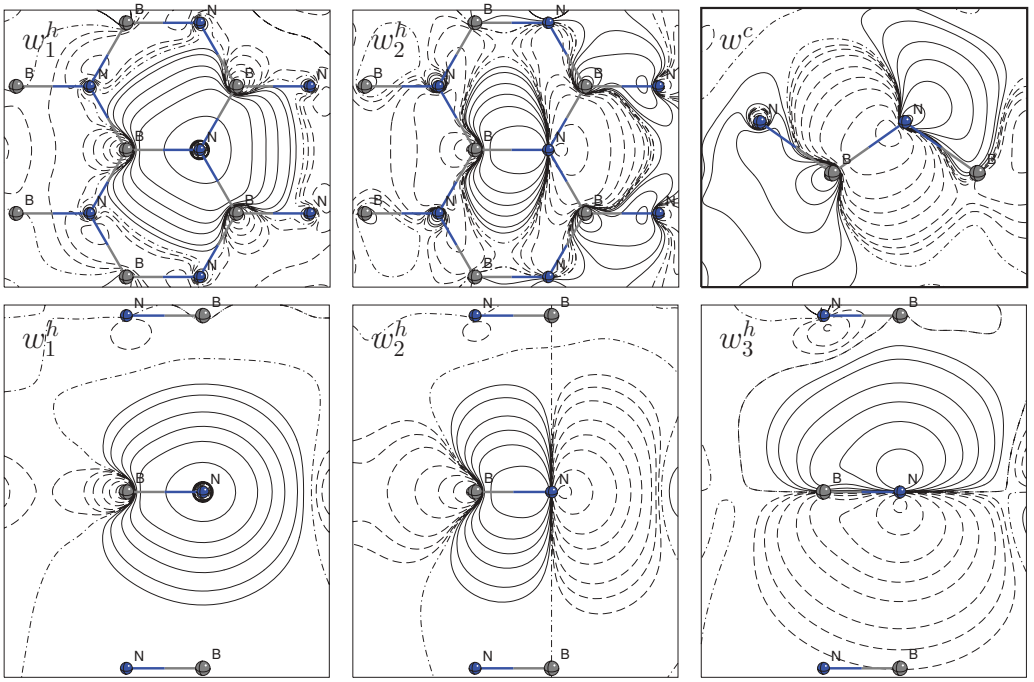

FIG. 2. (Color online) Plot of the symmetry-independent WFs for the two phases. For w^c (top right panel) a section in the (110) plane is shown, which includes the B-N bonds. For h-BN, two sections are provided, one in the basal layer (where w_3^h is zero), the other perpendicular to it (bottom plots). The distance between iso-amplitude lines is 0.01 a.u.; continuous, dashed, and dot-dash lines correspond to positive, negative, and zero values of the WFs, respectively.

the valence AOs of N, oriented along one of the B-N bonds, with some contribution from the corresponding AOs of the bonded B atom. Of the three WFs of h-BN, the most localized one, w_1^h, is mainly composed of the deep-lying s-type valence AOs on N; w_2^h is, on the contrary, the most diffuse, and forms with its partner a "two-petal flower,"[45] mainly resulting from a combination of p_x, p_y AOs of N with important contributions from the AOs of the neighboring B atoms; finally, w_3^h is essentially characterized as a p_z AO of N.

2. *Analysis and discussion of the MP2 results*

It is expedient to exploit the possibility offered by the local-correlation approach here adopted of analyzing the various contributions to the MP2 energy $E^{(2)}$, by quantifying the importance of the different pair energies $E_{ij}^{(2)}$ as defined in Sec. II B. These depend on the "type" of the two WFs (w_i, w_j) from which the two electrons are excited, and on the distance between the respective centers, $d_{ij} = |\mathbf{C}_i - \mathbf{C}_j|$, the latter, in turn, depending on the crystal cell where the second WF, w_j, is located, since the first one is always centered in the zero reference cell.

Figure 3 reports the values of $E_{ij}^{(2)}$ versus d_{ij} for the two phases in a log-log plot. With reference to the nomenclature used in Sec. III B 1, in c-BN there is only one type of pairs, while there are six in h-BN, identified by different symbols. In fact, when one or both of the WFs involved belongs to a "multipetal flower" (that is, it is classified according to a multidimensional irrep),[45] as it is the case of w_2^h, the average of the energies involving all petals in the same flower is taken and assigned to the average distance between the individual pairs.

The results for c-BN are similar to those obtained for the isostructural case of cubic silicon carbide.[57] All pair energies cluster around the ℓ_6 line which in a log-log plot corresponds to the London relationship ($E = -C_6 d^{-6}$) describing the interaction between two electronic systems separated by a (large) distance d. The spread is essentially associated to the different relative orientations of the interacting WFs.

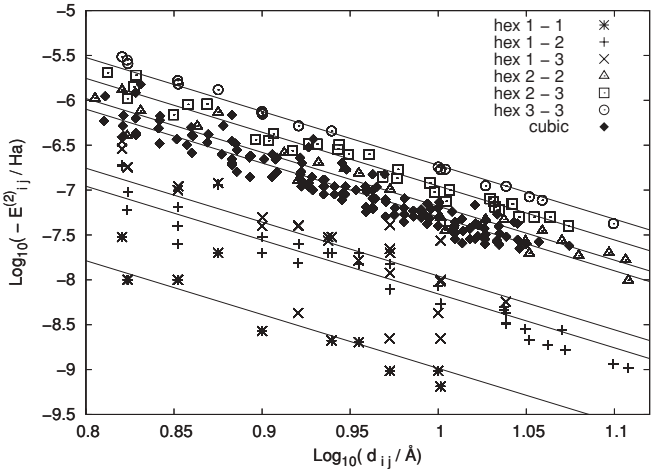

FIG. 3. Pair energies $E_{ij}^{(2)}$ vs distance d_{ij} in a log-log plot for the two BN phases. The different types of pairs are identified with different symbols, and the corresponding best-fit ℓ_6 lines are reported. For other explanations see text.

TABLE III. Values of the best-fit $C_{6(ij)}$ coefficients (mHa Å^6) for the different WF pairs and for the two basis sets, as indicated.

	h-BN						*c*-BN
(*ij*)	(11)	(12)	(13)	(22)	(23)	(33)	(11)
BSA	1.6	8.3	12.0	67.6	109.6	190.5	51.3
BSB	1.6	8.5	13.5	70.8	114.8	199.5	53.7

The case of *h*-BN is more interesting. Although on average the contributions are similar to those in *c*-BN, the spread of their importance is much wider. Excitations involving the *s*-like WF w_1^h are more than one order of magnitude less important than the other ones, which is clearly related to the much higher energetic cost needed to excite an electron from w_1^h (see Table II). For the same reason, the most effective electron-electron correlation interactions are those involving the p_z-like WF w_3^h. Interestingly, all the $E_{33}^{(2)}$ energies fall very close to the respective ℓ_6 line, independently of the fact that the two WFs belong or not to the same layer. Though individually less important, the p_x, p_y-like WFs w_2^h contribute on the whole the most to the correlation energy because of their double degeneracy.

The influence of the BS on long-range interactions can be checked by looking at the associate change of the London coefficient $C_{6(ij)}$ for the different WF pairs (see Table III). The increase is by about 4.5% for the most important pairs of the two phases. This is much less than the increase of the correlation energy by about 18% when passing from BSA to BSB as resulting from the data of Table I. This means that high-angular-momentum GTOs are especially important for describing short-range correlations (the Coulomb hole), whereas long-range correlation seems rather insensitive to them, as we have already noted in recent work on N_2 adsorbed on hexagonal BN.[58] As a matter of fact, the biggest effect is observed for the pair energies $E_{ii}^{(2)}$, corresponding to excitation of two electrons from the same localized orbital. Indeed, the Coulomb hole, where a correct description demands extended basis sets, is most pronounced for the opposite-spin close-by electrons, for which the two same-orbital electrons is the limiting case. In *c*-BN the gain in the correlation energy due to the larger basis set amounts to about 20%.

IV. CONCLUSIONS

The MP2 results compared to HF as well as PBE-*D* compared to PBE revert the order of the relative stability, correctly favoring the cubic phase. This indicates that long-range electron correlation is decisive for the relative stability of the BN polymorphs, thus the physically correct description of dispersion is crucial for evaluating this quantity. Moreover, it suggests that dispersion is not only important (as expected) for the layered *h*-BN, but even more so for the dense *c*-BN.

The MP2 method provides a reliable description of the electronic structure of the two BN phases, particularly so for the bigger basis set BSB. The virtually exact agreement of the MP2 cohesive energy with the experimental one is to some extent fortuitous, since at the basis set limit the discrepancy may be somewhat larger. However, since BSB is already a rather extended set, this discrepancy is not expected to be substantial. Indeed, as is well known from molecular calculations, MP2 is generally expected to provide rather accurate results for intermediately polarizable systems. The recent periodic applications,[36,37,59] including also this work, confirm this observation and support the usefulness of this method for estimating the relative stabilities of crystalline polymorphs. From the practical point of view, the density fitted local MP2 method allows for routine MP2 calculations with relatively big (triple-ζ) basis sets for crystals with small and moderate unit cells. Moreover, it can serve as a tool for analysis and partitioning of the interaction in chemically relevant terms.

For the DFT method, its intrinsic deficiencies become critical for the small energy differences involved here, rendering it incapable of providing a fully consistent and conclusive picture. The empirical *D* correction, on the other hand, although not guaranteeing high accuracy, might be useful for a qualitatively correct description, not only in the case of weakly bonded crystals. However, the empirical nature of this correction, especially the arbitrariness of the damping function, remains an issue.

ACKNOWLEDGMENT

The authors are grateful to Bartolomeo Civalleri for helpful discussions.

[1] R. H. Wentorf, J. Chem. Phys. **26**, 956 (1957).
[2] E. Rapoport, Ann. Chim. (Paris) **10**, 607 (1985).
[3] A. F. Goncharov, J. C. Crowhurst, J. K. Dewhurst, S. Sharma, C. Sanloup, E. Gregoryanz, N. Guignot, and M. Mezouar, Phys. Rev. B **75**, 224114 (2007).
[4] H. R. Philipp and E. A. Taft, Phys. Rev. **127**, 159 (1962).
[5] A. Rubio, J. L. Corkill, and M. L. Cohen, Phys. Rev. B **49**, 5081 (1994).
[6] X. Blase, A. Rubio, S. G. Louie, and M. L. Cohen, Europhys. Lett. **28**, 335 (1994).
[7] N. G. Chopra, R. J. Luyken, K. Cherrey, V. H. Crespi, M. L. Cohen, S. G. Louie, and A. Zettl, Science **269**, 966 (1995).
[8] E. Knittle, R. M. Wentzcovitch, R. Jeanloz, and M. L. Cohen, Nature (London) **337**, 349 (1989).
[9] V. L. Solozhenko and V. Z. Turkevich, J. Phys. Chem. B **103**, 2903 (1999).
[10] V. L. Solozhenko, High Press. Res. **13**, 199 (1995).
[11] E. Kim and C. Chen, Phys. Lett. A **326**, 442 (2004).
[12] W. J. Yu, W. M. Lau, S. P. Chan, Z. F. Liu, and Q. Q. Zheng, Phys. Rev. B **67**, 014108 (2003).
[13] T. E. Mosuang and J. E. Lowther, J. Phys. Chem. Solids **63**, 363 (2002).
[14] G. Kern, G. Kresse, and J. Hafner, Phys. Rev. B **59**, 8551 (1999).
[15] K. Albe, Phys. Rev. B **55**, 6203 (1997).
[16] J. Furthmüller, J. Hafner, and G. Kresse, Phys. Rev. B **50**, 15606 (1994).
[17] R. Ahmed, F. Aleem, S. J. Hashemifar, and H. Akbarzadeh, Physica B **400**, 297 (2007).

[18]M. Topsakal, E. Aktürk, and S. Ciraci, Phys. Rev. B **79**, 115442 (2009).
[19]A. Janotti, S. H. Wei, and D. J. Singh, Phys. Rev. B **64**, 174107 (2001).
[20]Y.-N. Xu and W. Y. Ching, Phys. Rev. B **44**, 7787 (1991).
[21]H. Rydberg, M. Dion, N. Jacobson, and E. Schroeder, Mater. Sci. Eng. C **23**, 721 (2003), e-print arXiv:cond-mat/0307017.
[22]G. K. H. Madsen, L. Ferrighi, and B. Hammer, Phys. Chem. Lett. **1**, 515 (2010).
[23]Y. Zhao and D. G. Truhlar, J. Chem. Phys. **125**, 194101 (2006).
[24]R. Demichelis, B. Civalleri, P. D'Arco, and R. Dovesi, Int. J. Quantum Chem. **110**, 2260 (2010).
[25]J. P. Perdew, A. Ruzsinszky, G. I. Csonka, O. A. Vydrov, G. E. Scuseria, L. A. Constantin, X. Zhou, and K. Burke, Phys. Rev. Lett. **100**, 136406 (2008).
[26]Y. Zhao and D. G. Truhlar, J. Chem. Phys. **128**, 184109 (2008).
[27]Z. Wu and R. E. Cohen, Phys. Rev. B **73**, 235116 (2006).
[28]C. Pisani, L. Maschio, S. Casassa, M. Halo, M. Schütz, and D. Usvyat, J. Comput. Chem. **29**, 2113 (2008).
[29]A. Erba and M. Halo, CRYSCOR09 User's Manual, Università di Torino, Torino, [http://www.cryscor.unito.it].
[30]P. Pulay and S. Saebø, Theor. Chim. Acta **69**, 357 (1986).
[31]M. Schütz, G. Hetzer, and H. J. Werner, J. Chem. Phys. **111**, 5691 (1999).
[32]H. Stoll, Phys. Rev. B **46**, 6700 (1992).
[33]A. Hermann and P. Schwerdtfeger, Phys. Rev. Lett. **101**, 183005 (2008).
[34]N. Gaston, B. Paulus, U. Wedig, and M. Jansen, Phys. Rev. Lett. **100**, 226404 (2008).
[35]S. J. Nolan, P. J. Bygrave, N. L. Allan, and F. R. Manby, J. Phys.: Condens. Matter **22**, 074201 (2010).
[36]L. Maschio, D. Usvyat, and B. Civalleri, CrystEngComm **12**, 2429 (2010).
[37]A. Grüneis, M. Marsman, and G. Kresse, J. Chem. Phys. **133**, 074107 (2010).
[38]J. Harl and G. Kresse, Phys. Rev. Lett. **103**, 056401 (2009).
[39]J. Paier, B. G. Janesko, T. M. Henderson, G. E. Scuseria, A. Grüneis, and G. Kresse, J. Chem. Phys. **132**, 094103 (2010).
[40]J. P. Perdew, K. Burke, and M. Ernzerhof, Phys. Rev. Lett. **77**, 3865 (1996).
[41]S. Grimme, J. Comput. Chem. **27**, 1787 (2006).
[42]C. Adamo and V. Barone, J. Chem. Phys. **110**, 6158 (1999).
[43]R. Dovesi *et al.*, *CRYSTAL09 User's Manual*, Università di Torino, Torino, [http://www.crystal.unito.it].
[44]C. M. Zicovich-Wilson, R. Dovesi, and V. R. Saunders, J. Chem. Phys. **115**, 9708 (2001).
[45]S. Casassa, C. M. Zicovich-Wilson, and C. Pisani, Theor. Chem. Acc. **116**, 726 (2006).
[46]L. Maschio and D. Usvyat, Phys. Rev. B **78**, 073102 (2008).
[47]M. Schütz, D. Usvyat, M. Lorenz, C. Pisani, L. Maschio, S. Casassa, and M. Halo, in *Accurate Condensed-Phase Quantum Chemistry*, edited by F. R. Manby (CRC, Taylor and Francis, New York, 2010), pp. 29–55.
[48]A. Grüneich and B. A. Hess, Theor. Chem. Acc. **100**, 253 (1998).
[49]J. T. H. Dunning, J. Chem. Phys. **90**, 1007 (1989).
[50]D. Usvyat, L. Maschio, C. Pisani, and M. Schütz, Z. Phys. Chem. **224**, 441 (2010).
[51]D. Usvyat, B. Civalleri, L. Maschio, R. Dovesi, C. Pisani, and M. Schütz, Approaching the theoretical limit in periodic MP2 calculations with atomic-orbital basis sets: the case of LiH (unpublished).
[52]M. Schütz, G. Rauhut, and H. J. Werner, J. Phys. Chem. A **102**, 5997 (1998).
[53]S. Boys and F. Bernardi, Mol. Phys. **19**, 553 (1970).
[54]H. J. Werner, P. J. Knowles, R. Lindh, F. R. Manby, M. Schütz *et al.*, MOLPRO: A Package of Ab Initio Programs, Version 2006.1 (2006), [http://www.molpro.net].
[55]K. Fuchizaki, T. Nakamichi, H. Saitoh, and Y. Katayama, Solid State Commun. **148**, 390 (2009).
[56]A. Malatesta, S. Fahy, and G. B. Bachelet, Phys. Rev. B **56**, 12201 (1997).
[57]C. Pisani, G. Capecchi, S. Casassa, and L. Maschio, Mol. Phys. **103**, 2527 (2005).
[58]M. Halo, S. Casassa, L. Maschio, C. Pisani, R. Dovesi, D. Ehinon, I. Baraille, M. Rérat, and D. Usvyat, Phys. Chem. Chem. Phys., doi:10.1039/C0CP01687J.
[59]M. Halo, S. Casassa, L. Maschio, and C. Pisani, Chem. Phys. Lett. **467**, 294 (2009).